Turning off cortical ensembles stops striatal Up states and elicits phase perturbations in cortical and striatal slow oscillations in rat *in vivo*

Fernando Kasanetz[1], Luis A. Riquelme[1], Patricio O'Donnell[2] and M. Gustavo Murer[1]

[1]*Departamento de Fisiología, Facultad de Medicina, Universidad de Buenos Aires, Buenos Aires, Argentina*
[2]*Center for Neuropharmacology and Neuroscience, Albany Medical College, Albany, NY 12208, USA*

***In vivo*, cortical neurons and striatal medium spiny neurons (MSN) display robust subthreshold depolarizations (Up states) during which they are enabled to fire action potentials. In the cortex, Up states are believed to occur simultaneously in a neuronal ensemble and to be sustained by local network interactions. It is known that MSN are impelled into the Up state by extra-striatal (primarily cortical) inputs, but the mechanisms that sustain and determine the end of striatal Up states are still debated. Furthermore, it has not been established if brisk perturbations of ongoing cortical oscillations alter rhythmic transitions between Up and Down states in striatal neurons. Here we report that MSN Up states terminate abruptly when persistent activity in cortical ensembles providing afferents to a given striatal region is turned off by local electrical stimulation or ends spontaneously. In addition, we found that phase perturbations in MSN membrane potential slow oscillations induced by cortical stimulation replicate the stimulus-induced dynamics of spiking activity in cortical ensembles. Overall, these results suggest that striatal Up states are single-cell subthreshold representations of episodes of persistent spiking in cortical ensembles. A precise spatial and temporal alignment between episodes of cortical persistent activity and striatal Up states would allow MSN to detect specific cortical inputs embedded within a more general cortical signal.**

(Received 8 May 2006; accepted after revision 23 August 2006; first published online 24 August 2006)
Corresponding author F. Kasanetz: Departamento de Fisiología, Facultad de Medicina, Universidad de Buenos Aires, Argentina. Paraguay 2155 7°, (1121) Buenos Aires, Argentina. Email: ferkasa@fmed.uba.ar

Episodes of persistent spiking occur in the cerebral cortex, basal ganglia, thalamus, brainstem and spinal cord, and may contribute to short-term storage of information, modulation of neural responses by attention, and maintenance of sleep-related activity (Steriade, 2000; Major & Tank, 2004; Yuste *et al.* 2005). Cortical persistent activity is perceived as a local network phenomenon: balanced excitatory and inhibitory local interactions, neuromodulators and intrinsic cellular mechanisms sustain cortical neurons in a near-threshold condition termed Up state (Lewis & O'Donnell, 2000; Sanchez-Vives & McCormick, 2000; Timofeev *et al.* 2000; Shu *et al.* 2003; Tseng & O'Donnell, 2005). Striatal medium spiny neurons (MSN) also show persistent activity in the form of Up states. It is well known that extra-striatal (primarily cortical) excitatory inputs impel MSN into the Up state (Wilson, 1993; O'Donnell & Grace, 1995) and local connectivity, neuromodulators, and MSN intrinsic conductances may be important for Up state maintenance (Hernandez-Lopez *et al.* 1997; Czubayko & Plenz, 2002; Blackwell *et al.* 2003; Vergara *et al.* 2003; Wolf *et al.* 2005). It is also known that the oscillatory nature of Up–Down alternation in the striatum is correlated with similar oscillations in cortical areas providing the majority of afferents to a given striatal region (Charpier *et al.* 1999; Mahon *et al.* 2001; Tseng *et al.* 2001; Goto & O'Donnell, 2001). During cortical field potential activation (i.e. epochs with dominant high frequency components), dorsal striatal oscillations are replaced by steadier, non-rhythmic Up states (Kasanetz *et al.* 2002). As it has been proposed that a neuromodulatory action of dopamine on MSN voltage- and NMDA-dependent calcium currents may prolong striatal Up states beyond the action of extra-striatal excitatory inputs (Hernandez-Lopez *et al.* 1997; Suri *et al.* 2001; Gruber *et al.* 2003; Vergara *et al.* 2003) and corticostriatal projections are to some extent topographically organized (Voorn *et al.* 2004), it remains to be established to what extent episodes of persistent cortical activity and striatal Up states can display separate dynamics *in vivo*.

The above studies established that subthreshold MSN oscillations are modulated by global brain dynamics.

 DOI: 10.1113/jphysiol.2006.113050

However, the precise temporal pattern of cortical control of MSN Up states remains to be clarified. An electrical pulse applied to the cerebral cortex *in vivo* evokes a stereotyped MSN response consisting of a depolarizing postsynaptic potential (dPSP) followed by a long-lasting hyperpolarization (LLH) and a late depolarization (LD). The LLH is thought to be caused by a reduction of cortical input (Wilson *et al.* 1983), but this has never been conclusively demonstrated. As recent studies show that cortical persistent activity may be turned on and off by local electrical stimulation in slices (Shu *et al.* 2003), it is possible that cortical stimulation *in vivo* induces a similar phenomenon. Here we explored the temporal and spatial dynamics of the cortical control of striatal Up states by recording for the first time cortical field potentials and cortical spiking activity through multichannel electrodes together with the membrane potential of MSN that receive inputs from specific cortical locations. We further examined whether brisk phase perturbations of ongoing cortical rhythms induced by local electrical stimulation affected cortical and striatal network synchrony.

Methods

Animal preparation

Adult male Sprague-Dawley rats ($n = 22$) were maintained on a 12 : 12 h light–dark cycle with food and water available *ad libitum,* and were cared for in accordance with local institutional regulations on the use of laboratory animals (Servicio Nacional de Sanidad y Calidad Agroalimentaria, RS 617/2002, Argentina). On the day of the experiment, rats (weight, 300–450 g) were anaesthetized with urethane (1.2–1.5 g kg^{-1}, I.P.), treated with a local anaesthetic on the scalp (bupivacaine hydrochlorate solution, 5% w/v, Duracaine, AstraZeneca S.A. Argentina, 0.1–0.3 ml, S.C.) and pressure points (lidocaine hydrochlorate gel, 2% w/w, Denver Farma S.A. Argentina), and secured to a stereotaxic frame (Stoelting, Wood Dale, IL, USA). Temperature was maintained at 36–37°C with a servo-controlled heating pad (Fine Science Tools, Vancouver, Canada). Additional urethane was administered throughout the experiment as necessary in order to maintain a constant level of anaesthesia, as determined from cortical field potential recordings and evaluation of the hindlimb withdrawal reflex (customarily, supplements of 0.3–0.4 g kg^{-1} S.C. every 3–4 h) (Kasanetz *et al.* 2002). At the end of the recording session, rats received a lethal dose of urethane and were transcardially perfused with cold saline followed by 4% paraformaldehyde in phosphate buffered saline (PBS). Brains were removed, stored overnight in the same fixative, and then incubated in 0.1 M PBS containing 15% sucrose for 24–48 h. The localization of extracellular recording and stimulation sites was determined from Nissl-stained sections.

Cortical recording and stimulation

In most rats ($n = 17$), three concentric bipolar electrodes (SNE-100, Better Hospital Equipment, New York, USA; outer contact diameter 0.25 mm, exposure 0.25 mm; central contact protrudes 0.75 mm from outer contact, has 0.1 mm in diameter and 0.25 mm tip exposure) were used to obtain differential electrocorticogram (ECoG) recordings from separate cortical regions: the medial frontal prelimbic cortex (3.5 mm anterior to bregma, 0.5 mm lateral to midline and 4 mm below the cortical surface, 20 deg angle in the sagittal plane; Paxinos & Watson, 1997), motor cortex (3.5 mm anterior to bregma, 2.5 mm lateral and 2.5 mm below cortical surface, 20 deg angle in the sagittal plane) and primary somatosensory cortex (2.8 mm posterior to bregma, 6.5 mm lateral and 2 mm below cortical surface, positioned with a 20 deg angle in the coronal plane; Fig. 1*A* and *C*). Three additional bipolar electrodes each consisting of two Teflon-coated tungsten wires (50 μm tips; vertical tip separation of ∼0.5 mm) were located at a distance of ∼0.5 mm from each ECoG recording site. Stimulation consisted of 0.5 mA square wave pulses of 0.3 ms duration at 0.5 Hz or 0.16–0.25 Hz. The cortical field potential was amplified (ER-98, NeuroData, Delaware Water Gap, PA, USA; Lab1, Akonik, Argentina), band-pass filtered (0.1–300 Hz), and sent to an analog-to-digital converter (DigiData 1322A, Axon Instruments, Union City, CA, USA). In some rats ($n = 5$), cortical recordings were obtained with a 16-channel, four-shank silicon probe (200 μm vertical site spacing and 200 μm horizontal shank spacing, kindly provided by The University of Michigan Center for Neural Communication Technology). The array was orientated in the coronal plane with a 20 deg lateral angle and positioned ∼0.5 mm posterior to the motor cortex ECoG recording/stimulation site (no electrodes were located in the prelimbic or somatosensory cortices in these experiments). These signals were amplified, filtered (0.3–3 kHz), and digitized at 10 kHz (DigiData 1200, Axon Instruments).

Striatal intracellular recording

Intracellular recordings were obtained as previously described (Tseng *et al.* 2001; Kasanetz *et al.* 2002) from one of the following striatal regions (ipsilateral to the ECoG recordings): anterior dorsolateral striatum (0.5–1 mm anterior to bregma, 3–4 mm lateral, 3–5 mm below the cortical surface; 8 recorded neurons), medial striatum (+0.4 to −0.2 mm relative to bregma, 2–2.5 mm lateral and 3–5 mm below the cortical surface; 8 neurons) or posterior dorsal striatum (1.4–2 mm posterior to bregma, 4–5 mm lateral and 3–5 mm below the cortical surface; 5 neurons) (Fig. 1*B*). These striatal regions were paired with the three cortical stimulation/recording sites (anterior

dorsolateral striatum with motor cortex, medial striatum with prelimbic cortex and posterior dorsal striatum with somatosensory cortex; Voorn *et al.* 2004). In addition, another nine neurons were recorded in the anterior dorsolateral striatum together with MU activity in the motor cortex. In order to ascertain that the recorded striatal neuron received inputs from the matched cortical region, cortical stimulation was used to verify an evoked monosynaptic dPSP in the striatal neuron. All ECoG–MSN pairs analysed in the present work met these anatomical and physiological criteria. Intracellular microelectrodes were filled with 2 M potassium acetate and 2% Neurobiotin (RBI, Natick, MA, USA), and had a resistance ranging from 60 to 130 MΩ. The signal was sent to a bridge amplifier (Axoclamp 2B, Axon Instruments) and digitized at 10 kHz (DigiData 1322A, Axon Instruments). Microelectrodes were slowly advanced through the striatum with a hydraulic micromanipulator until a neuron was impaled. After completion of experimental procedures, neurons were labelled with Neurobiotin (Kita & Armstrong, 1991).

Signal analysis

Cortical and striatal activities evoked by a single cortical stimulus can be divided into early and late components. The early components include an abrupt positive wave in the ECoG and a dPSP in the intracellular MSN

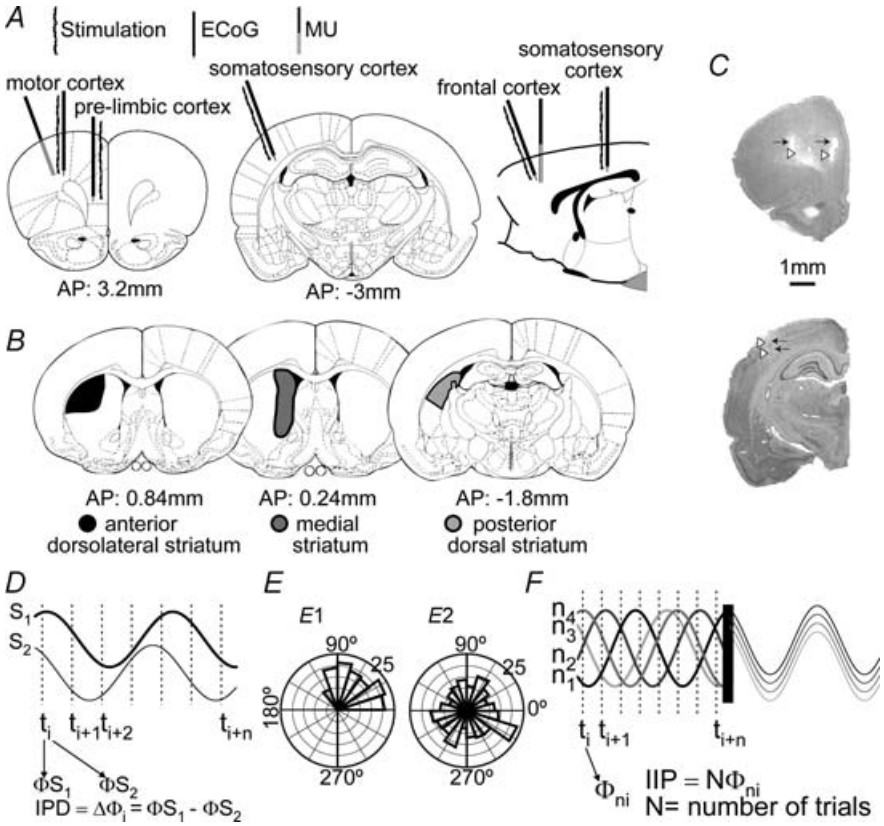

Figure 1. Simultaneous cortical and striatal recordings
Schematic drawings of coronal and sagittal brain sections (Paxinos & Watson, 1997) displaying the position of cortical (*A*) and striatal (*B*) recording and stimulation sites. *C*, photographs of Nissl-stained sections depicting tracks of recording (white arrowheads) and stimulation (black arrows) electrodes in cortical structures. *D*, instantaneous phase differences (IPD) between two signals were calculated for every sampling interval during a defined time window. The dispersion of IPD circular distribution was taken as an index of coupling. Here, two sinusoidal waveforms were used to illustrate how IPDs were computed. Note that this does not mean that slow waves are sinusoidal (real slow waves can be seen in Fig. 2). *E*, throughout this paper, data are represented in circular distributions. Here, two polar plots illustrate prototypical uniform (right) and non-uniform (left) circular distributions. *F*, in order to estimate stimulus phase locking for a number of stimulation trials (*N*), trials were aligned to the stimulus time and instantaneous phases at any sampling interval along *N* trials were computed. This is illustrated here with overlapping episodes of an artificial sinusoidal waveform. The circular distribution of instantaneous phases at a given post-stimulus time (IIP: intertrial instantaneous phase) should be non-uniform if there is stimulus locking. Φ_i, instantaneous phase; Φ_{ni}, instantaneous phase of individual trial; t_i, sampling interval; n_i, trial number; *N*, number of trials.

recordings. The late components include a slow wave with an initial negative phase in the ECoG and a LLH–LD sequence in striatal MSN. Through this report we will solely consider the late components and their relation to cortico-basal ganglia network dynamics. For all subsequent analyses, recordings were grouped according to the ongoing cortical network activity state at the time of electrical stimulation, as shown by the ECoG. Epochs with obvious ongoing cortical slow waves or notorious activation were selected by careful visual inspection of the signals. During spontaneous activity, cortical activation results in a marked drop of the ratio between relative powers in the low (≤ 2 Hz) and high (> 2 Hz) frequency ranges of the ECoG power spectrum (see Kasanetz *et al.* 2002 for more details). Throughout periods of electrical stimulation, the presence of ongoing slow waves or cortical activation could be visually discerned during pre-stimulus periods. Ongoing cortical activation was evident as a significant decrease of the power of low frequency ECoG components in pre-stimulus epochs compared with epochs of similar length recorded during spontaneous slow wave activity in the same neuron.

Concomitant MSN and ECoG activities were studied in recording epochs that included the 1 s preceding and the 1 s following the stimulus (25–90 consecutive trials). To simplify the analysis, each successive group of N points in the signals was averaged to yield a single point that was retained, allowing sampling reduction to 1000 Hz (Axoscope). A discrete wavelet transformation of the signals (Meyer, 1992), was performed by means of a finite impulse response (FIR) digital filter approximation of the Meyer wavelet function (MatLab, The MathWorks, Inc., Natick, MA, USA). The procedure is based on an iterative algorithm that filters and down-samples the signal during each iteration. Down-sampling is performed by dyadic decimation, so the maximal number of iterations, or decomposition levels, is given by $\log2(N)$, with N being the length of the signal (number of sampled points). Briefly, the signal is first convoluted with the FIR filter and then down sampled, providing $N/2$ approximation coefficients (cAi; a representation equivalent to low pass filtering the signal) and $N/2$ detail coefficients (cDi; retaining information of frequencies above the filter cut-off frequency). In the next iteration, the cAi vector (instead of the signal) is subjected to filtering and down-sampling to obtain cAi + 1 and cDi + 1. From pairs of cAi and cDi vectors, the waveforms from which they were obtained (and ultimately the signal) can be reconstructed by iterative up-sampling and filtering. If zeros are used instead of the cAi vectors during reconstruction, the resulting waveforms are equivalent to band-passed versions of the original signal, the frequency content of which is determined by the decomposition level. The waveforms retaining information of the 0.5–2 Hz components of the signals were chosen to study transitions between active and silent cortical states and Up and Down striatal states, because the main frequency of these oscillations is ∼1 Hz (Stern *et al.* 1997; Steriade, 2000; Kasanetz *et al.* 2002).

In order to assess the degree of coupling between MSN membrane potential (V_m) and ECoG, we first computed cross-correlograms for delays of 0.75 s with a resolution of 1 ms for both pre- and post-stimulus 1 s epochs. Cross-correlograms of successive trials were averaged to obtain a mean correlation coefficient for each MSN–ECoG pair. The significance of cross-correlations for individual neurons was determined by contrasts against surrogate data. An additional estimate of synchronization was provided by the stability (or, conversely, the dispersion) of the phase lag between signals (Fig. 1*D*). Instantaneous phases ($\phi_{MS^{Ni}}$ and ϕ_{ECoGi}) were calculated as the phase angle of the Hilbert-transformed and normalized (−1 to 1) waveforms (Oppenheim *et al.* 1999), and the instantaneous phase differences (IPD; $\Delta\phi_i = \phi_{MS^{Ni}} - \phi_{ECoGi}$) were depicted in circular distributions (Fig. 1*E*). These distributions were characterized by a mean direction and a circular dispersion, which were calculated as follows (Fisher, 1993):

$$\text{mean direction } (\theta):\ \theta = \tan^{-1}(S/C)$$

where $S = \Sigma \sin(\Delta\phi_i)$ and $C = \Sigma \cos(\Delta\phi_i)$

$$\text{circular dispersion}(\delta):\ \delta = (1 - m_2)/(2R^2)$$

where $m_2 = 1/N\ \Sigma(\cos(2\,(\Delta\phi_i - \theta))$, and $R^2 = (C^2 + S^2)/N$.

To seek for phase resetting of ongoing slow rhythms, stimulation trials were aligned at stimulus onset. Then, for each millisecond and waveform we grouped ϕ_i (calculated with the Hilbert transform) across trials, obtaining samples of N intertrial instantaneous phases (IIP), where N is the number of trials (Fig. 1*F*). We considered IIP constancy as an index of stimulus phase locking. To estimate IIP variability, we computed the probability for IIP distributions to be uniform by means of the Rayleigh test (Fisher, 1993), and computed their circular dispersion (δ) as mentioned above. In addition, LD latency stability was taken as an index of phase locking. The LD latency was established as the post-stimulus time at which the normalized (−1 to 1) wavelet transformed signals first crossed zero with a positive slope during the late response. Similarly, spontaneous transitions between Down and Up states were detected as zero crossing with a positive or negative slope (Down-to-Up and Up-to-Down, respectively) in the 0.5–2 Hz wavelet transformed V_m of recordings with dominant slow waves. In order to make analogous computations on cortical multi-channel multiunit recordings, MU signals were first rectified. Then, a single waveform was obtained by adding, for every sampling interval, all simultaneously recorded MU channels. Finally, the resulting waveform was smoothed

by averaging along a 50 ms sliding window to obtain a single representation of multiunit activity (MUras). The 0.5–2 Hz components were extracted with wavelet and Hilbert procedures, as described above.

Results

The dynamics of cortical and striatal persistent activity were examined with intracellular recordings from dorsal striatal MSN conducted simultaneously with cortical local field potentials (ECoG) and multiunit activity of cortical neurons in urethane-anaesthetized rats (Fig. 1). Cortical neuron action potential firing occurs during the positive portion of the field potential slow waves (Fig. 2). Throughout this paper, the terms cortical active and silent states will refer to periods of cortical ensemble firing and absence of firing, respectively, which alternate periodically, originating ECoG slow waves. The terms Up and Down states will exclusively be used to name MSN V_m states. Spontaneous alternation between Up and Down states, synchronous with the cortical slow waves, was apparent in all recorded MSN ($n = 30$; Table 1) (slow oscillation frequency (Hz): 0.91 ± 0.04 and 0.92 ± 0.05 for MSN V_m and ECoG, respectively; mean $\pm$ S.E.M.). MSN two-state transitions lagged behind ECoG slow waves by 34 ± 23 ms (mean $\pm$ S.E.M.). The V_m of a few MSN preceded or was simultaneous with cortical slow waves in the matching cortical region, suggesting that other cortical regions may contribute to triggering transitions between Up and Down states. Up states occurred during the active (positive) portion of the cortical slow waves (Fig. 2). Many recordings displayed spontaneous disruptions of the cortical slow oscillation ('activation'), lasting from seconds to a few minutes, which were invariably associated with persistent cortical firing and sustained MSN depolarization (Fig. 2). Thus, as previously shown (Kasanetz *et al.* 2002), MSN Up and Down states follow ongoing cortical activity.

Cortical stimulation transiently resets ongoing slow oscillations in both cortical networks and striatal medium spiny neurons

Electrical cortical stimulation at ~0.5 mm from cortical recording sites evoked a short latency dPSP in MSN located in the matched striatal region followed by a slow V_m modulation consisting of a hyperpolarization lasting about 350 ms (LLH) and a robust depolarization (LD) (Fig. 3; Table 1). As previously reported (Tseng *et al.* 2001, 2004), the LLH–LD sequence ('late response') closely resembled spontaneous Down-to-Up state transitions. The MSN late response was associated with an evoked ECoG slow wave, with an initial negative (silent) part. In addition, after stimulation of a non-matched cortical region, many MSNs responded with a dPSP (usually of smaller amplitude) and a largely more variable LLH–LD sequence (even in the case when no dPSP was observed). Non-matched delayed responses were not systematically analysed and will not be further discussed here (see Supplementary Fig. 1 for more details and a brief discussion).

Cortical stimulation induced cortical and striatal late responses regardless of the ongoing cortical activity state (Fig. 3). For recordings displaying an ongoing ECoG dominated by slow waves ($n = 13$), we computed cross-correlations between the ECoG and MSN V_m for the 1 s signal segments that preceded and followed the stimulus (interstimulus interval: 2 s). Peak correlation coefficients were always highly significant (typically higher than 0.7) both before and after stimulus arrival (Fig. 4*A*). Another estimate of synchronization, the stability of

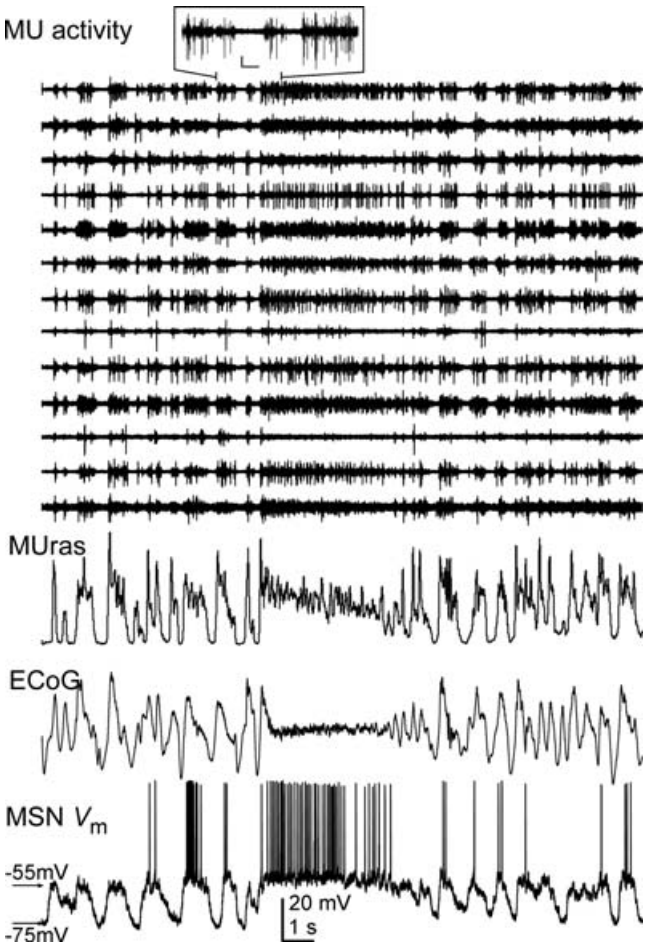

Figure 2. Correlated spontaneous cortical and striatal activity
Simultaneous recordings of the electrocorticogram (ECoG) and multiunit activity (MU) from deep layers of the motor cortex (selected MU channels are displayed). The activity from channels displaying clearly visible spikes was rectified, added and smoothed to obtain the trace labelled MUras. MUras closely resembles the ECoG. Inset: detail of MU activity; calibration bars: 0.25 mV, 0.2 s. Amplitudes were normalized for ECoG and MUras. MU activities were scaled individually to allow better visualization of the signals.

Table 1. Electrophysiological properties of striatal medium spiny neurons

Action potential amplitude[a]	42.6 ± 1 mV	
Membrane potential, Down (mV)	86.1 ± 2.1	
Membrane potential, Up (mV)	72.4 ± 2.2	
Input resistance [b] (MΩ)	56.1 ± 3.7	
dPSP amplitude (mV)	12.6 ± 1.8	
dPSP latency (to the peak) (ms)	18.0 ± 0.9	
Late response to cortical stimulation	Slow wave ECoG	Activated ECoG
Long latency hyperpolarization duration (ms)	396 ± 35[c]	290 ± 32
Late depolarization latency (ms)	439 ± 33	340 ± 32
Coefficient of variation of late depolarization latency	0.41 ± 0.03[d]	0.20 ± 0.05

[a]Measured from threshold; [b]measured during the Down state by applying hyperpolarizing current pulses (see Tseng *et al.* 2001 for details). Data are mean ± S.E.M. [c] $P = 0.05$, [d] $P = 0.003$, *versus* activated ECoG condition, *t* test.

phase differences between the signals, revealed that the circular distributions of instantaneous phase differences (IPD) were as narrow for the 1 s preceding as for the 1 s following the stimulus (IPD circular dispersion: pre-stimulus: -0.92 ± 0.08; post-stimulus: -0.92 ± 0.10; log mean ± S.E.M.; Fig. 4*B*). Estimation of phase lags indicated that MSN late responses lagged behind cortical slow waves by 27 ± 22 ms. Further analyses revealed that the power of the dominant low frequency components of the late response was not modified by stimulation, neither in the ECoG nor in MSN V_m, when background ECoG was dominated by slow waves (Fig. 4*C*). Polar plots depicting the relative amplitudes of the MSN V_m and ECoG (radial axis) as a function of ECoG phase (angular axis) (Fig. 4*D*) and of IPD as function of ECoG phase (not shown) indicated that IPD was conserved throughout spontaneous Up states and LD. To rule out the possibility that evoked responses were entrained by the repeated stimulation, we repeated this analysis on recordings taken with longer inter-stimulus intervals (4–6 s; $n = 6$) and found similar results (correlation coefficients: 0.76 ± 0.03 and 0.71 ± 0.05; IPD circular dispersion: -0.84 ± 0.12 and -0.94 ± 0.16; for pre- and post-stimulus epochs, respectively, $P > 0.5$ *versus* 2 s inter-stimulus interval data, paired *t* test).

The above results indicate that MSN V_m is tightly locked to cortical slow wave activity and that this tight coupling is not modified by cortical stimulation. Therefore, it is conceivable that once fast events subside, Up states shift back to what is determined by the global cortical activity. Visual inspection of stimulus-aligned trials suggests that late responses are time-locked to the stimuli (Fig. 5*A*). To determine whether cortical stimulation resets ongoing slow rhythms, we computed the instantaneous phase of ECoG and MSN V_m low frequency components, aligned all stimulation trials in a given neuron at stimulus onset, and analysed intertrial instantaneous phase (IIP) distributions for the 1 s periods preceding and following

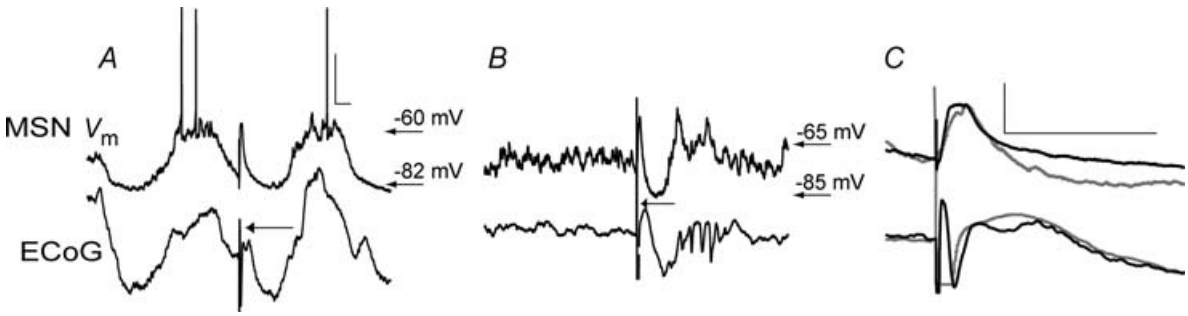

Figure 3. Cortical and striatal activities respond to cortical stimulation
Typical responses of MSNs and the cortical field potential to stimulation of deep layers of the cerebral cortex at less than 1 mm from the cortical recording site (500 μA). Responses exhibit roughly similar temporal courses independently of the ongoing global brain activity state (*A*, slow wave state; *B*, activated ECoG state). Traces in *A* and *B* correspond to two different neurons. *C*, the short latency response to cortical stimulation of the MSNs displayed in *A* (black) and *B* (grey), consisting in dPSPs (above), are displayed with the concomitant ECoG wave (below). Scale bars: 20 mV (V_m), 0.3 mv (ECoG), 100 ms.

the stimuli (Fig. 5*B*). Since the stimulus could arrive at any phase of the ongoing slow wave, IIPs should be distributed uniformly before the stimulus arrives, and if the stimulus resets the slow wave, the IIPs should conversely display a restricted distribution and reduced variability for a period of time (Makeig *et al.* 2002; Fell *et al.* 2004; Shah *et al.* 2004). As expected, polar plots revealed highly variable IIPs with nearly uniform IIP distributions at any pre-stimulus time, both for V_m and ECoG, but condensed non-uniform IIP distributions with very low variability at any given post-stimulus time (Fig. 5*D* and *E*). Both the probability for IIP distributions to be uniform (Rayleigh test) and the circular dispersion of IIP distributions (Fig. 5*D*) dropped markedly following the stimulus (Rayleigh probability, mean ± S.E.M. pre-stimulus: MSN, 0.12 ± 0.06; cortex, 0.12 ± 0.05; post-stimulus: MSN, 0.02 ± 0.01, $P < 0.004$; cortex, 0.007 ± 0.006, $P < 0.006$, Wilcoxon paired test; IIP distribution circular dispersion: log mean ± S.E.M. pre-stimulus: MSN, 1.00 ± 0.11; cortex, 0.91 ± 0.13; post-stimulus: MSN, 0.32 ± 0.16, $P < 0.001$; cortex, 0.17 ± 0.13, $P < 0.0003$, paired t test, $n = 13$). All six ECoG–MSN paired recordings tested with longer inter-stimulus intervals provided similar results (Rayleigh probability: MSN V_m: 0.19 ± 0.13 and 0.0001 ± 0.0001; ECoG: 0.14 ± 0.09 and 0.001 ± 0.004; mean ± S.E.M. of pre- and post-stimulus epochs, respectively; IIP distribution circular dispersion: MSN V_m: 1.36 ± 0.16 and 0.02 ± 0.19; ECoG: 1.29 ± 0.08 and 0.03 ± 0.22; log mean ± S.E.M. of pre- and post-stimulus epochs, respectively; no value differed significantly from the

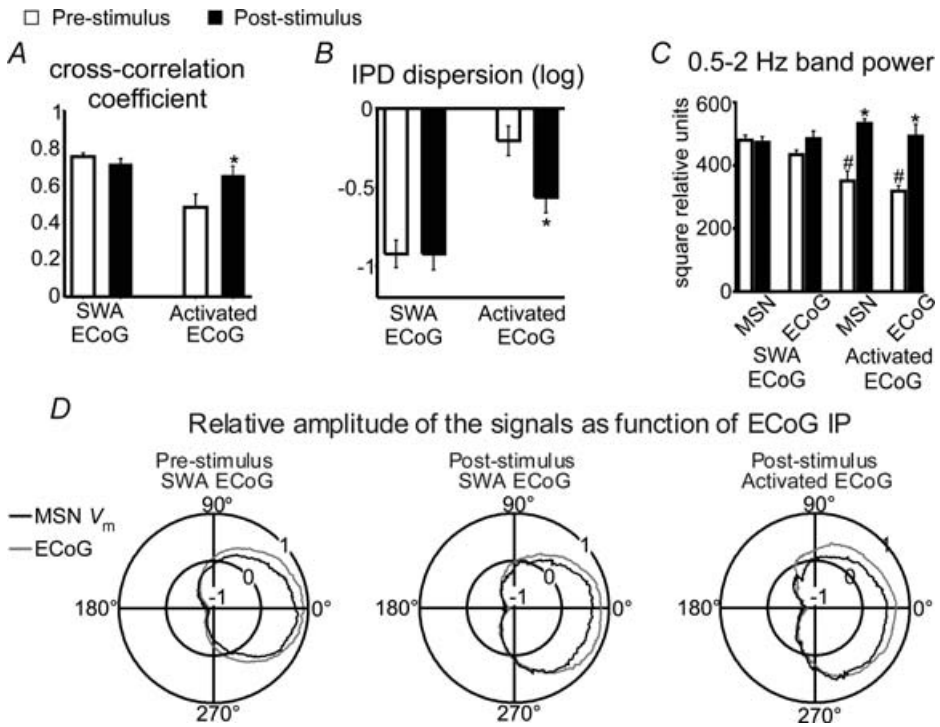

Figure 4. Effects of cortical stimulation on corticostriatal coupling
The effect of cortical stimulation on the degree of coupling between the ECoG and MSN membrane potential was estimated by computing pre- and post-stimulus cross-correlograms and instantaneous phase differences (IPD). In the slow wave activity background condition (SWA ECoG), peak cross-correlation coefficients (*A*) and IPD circular dispersion (*B*) did not significantly differ between before and after stimulation (paired t test, $n = 13$). Conversely, in the activated ECoG condition (activated ECoG), peak cross-correlation coefficients increased ($^*P < 0.006$) and IPD circular dispersion decreased ($^*P < 0.01$) compared with pre-stimulus values ($n = 8$, paired t test), indicating that cortical stimulation enhanced low frequency coupling between cortical and striatal activity. For individual neurons, pre-stimulus cross-correlations in the SWA background condition were significant at $P < 0.001$ and non-significant for the activated ECoG background condition. *C*, cortical stimulation had no effect on ECoG or MSN membrane potential power when background activity was dominated by slow waves, but increased significantly low frequency signal components in both areas when background activity was activated ($^*P < 0.001$ *versus* pre-stimulus condition, $n = 8$, paired t test). Both the ECoG and MSN V_m powers were significantly smaller in the activated ECoG condition compared with the SWA background ($^\#P < 0.001$, t test). *D*, polar plots depicting mean relative amplitudes (radial axis: −1 to +1) of MSN membrane potential (black) and ECoG (grey) as a function of ECoG instantaneous phase (IP) (angular axis: 0 to 360 deg). Signal amplitudes changed in parallel, with transitions from silent to active states taking place at ∼270 deg phase, both during spontaneous activity or after cortical stimulation and regardless of the background ECoG condition.

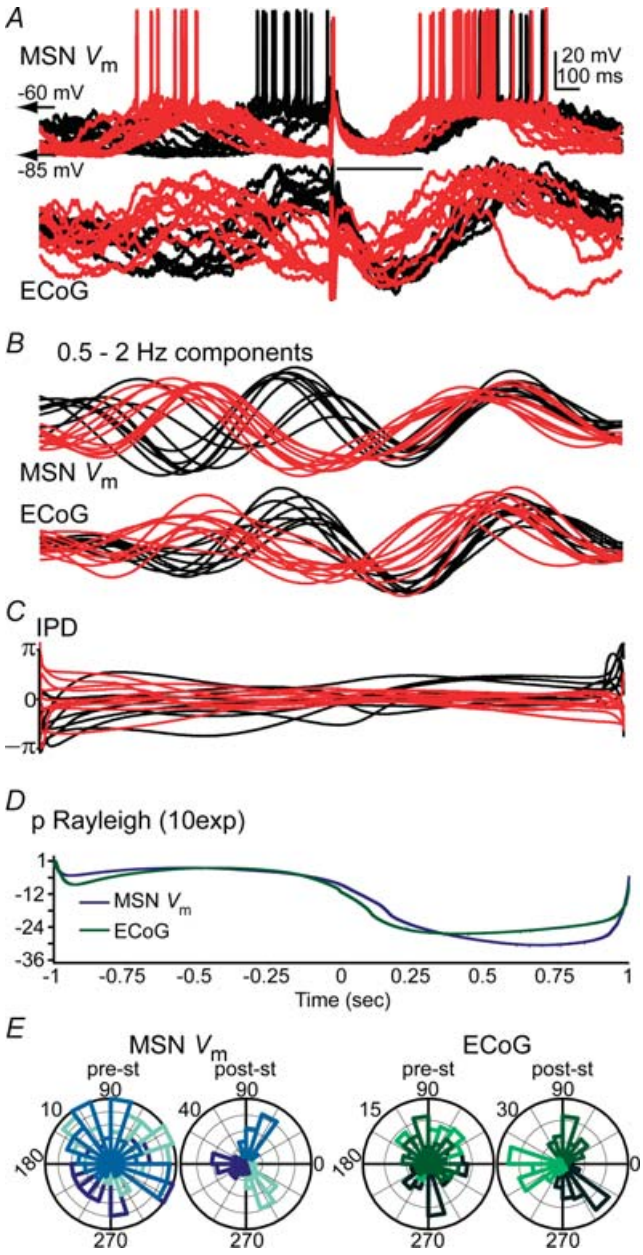

Figure 5. Cortical stimulation transiently resets ongoing cortical and striatal slow oscillations
A, twenty responses to cortical stimulation of a MSN–ECoG pair were selected from a total of 90 trials, to illustrate the effect of electrical pulses delivered during either silent (red trials) or active (black trials) corticostriatal states. Trials were aligned at stimulus onset. MSN Up states came invariably to an end regardless of the time spent in the Up state prior to stimulus arrival. The arrow points to the stimulus artifact; its module is the late depolarization mean latency. *B*, the elementary features of the slow oscillation were preserved in the 0.5–2 Hz components, which were isolated with wavelet decomposition. *C*, the instantaneous phase of MSN membrane potential and ECoG slow oscillations was computed with a Hilbert transformation. The instantaneous phase difference (IPD) between the signals was preserved throughout the 2 s inter-stimulus interval (see Fig. 4 for population data). *D*, we computed inter-trial instantaneous phase (IIP) distributions throughout the 2 s inter-stimulus interval with 1 ms resolution and the probability for each of these distributions to be uniform by means of the Rayleigh test. For the representative MSN–ECoG pair depicted above, the Rayleigh probability markedly dropped post-stimulus, indicating that cortical stimulation deviated IIP distributions from uniformity. This stimulus-induced inter-trial phase concentration is indicative of a phase resetting effect of cortical stimulation on both signals. *E*, polar histograms displaying pre- and post-stimulus IIP distributions (pre-st and post-st, respectively; radial axis, number of events) of the MSN membrane potential (left) and ECoG (right). Each plot includes three IIP distributions, corresponding to different pre- or post-stimulus times, where the different IIP distributions are depicted in different tones. The tones are widely spread throughout the phase space for pre-stimulus times, producing an overlapping pattern in the polar plot, because pre-stimulus IIP distributions were uniform. Conversely, for the post-stimulus times the tones are concentrated at specific phase angles (angular axis), indicating that the slow wave had a similar phase in the different trials at any given post-stimulus time. All data are from the same MSN.

corresponding 2 s interstimulus interval value, Wilcoxon rank sum test). Thus, cortical stimulation transiently perturbs ongoing slow cortical and striatal activities.

A 2 s inter-stimulus interval could mask the transient nature of coherent cortical and striatal activities. IIPs of the slow wave at the time of stimulus arrival were distributed uniformly, suggesting that the phase shifting effect of the stimulus was short lived. However, the inherent variability of the slow oscillation could have caused a seemingly short-lived phase shifting effect of cortical stimulation. To examine the latter possibility, we aligned 4-s-long segments of spontaneous slow wave activity following cortical stimulation (Fig. 6*A*) or a spontaneous Down-to-Up state transition (Fig. 6*B*), and computed, for every millisecond, the probability for IIP distributions to be uniform. Rayleigh probability increased to non-significant values in less than 2 s after the aligning tag (Fig. 6*C*). We established the time to a 50% increase in Rayleigh probability as the duration of the 'phase shifting effect', comparing the effects of cortical stimulation with artificially aligning spontaneous activity. Typical phase shift durations were ∼1 s and were not significantly different between both conditions (Fig. 6). This suggests that cortical stimulation exerts a short-lived phase shift in cortical and striatal dynamics that can be explained by the slow oscillation inherent variability.

Cortical stimulation induces cortical and striatal slow waves regardless of the ongoing cortical activity state

The above results indicate that the main effect of cortical stimulation on local networks and the MSN V_m is a concerted phase perturbation of ongoing slow oscillations. However, cortical stimulation delivered during ECoG activation ($n = 8$) produced an ECoG slow wave and a LLH followed by a LD with an almost fixed latency in all recorded MSN (Fig. 7*A*). In these cases, there was a low pre-stimulus ECoG–MSN V_m cross-correlation at

the dominant low frequency of the late response that increased significantly following stimulation (see Fig. 4*A*). Phase lag variability, as assessed by computing IPD circular dispersion, was very high before the stimulus and decreased significantly post-stimulus (Fig. 4*B*). Indeed, the degree of coupling between evoked cortical and striatal waveforms was as strong in the activated ECoG condition as in the slow wave background condition (Fig. 4). This result further indicates that cortical stimulation affects cortical and striatal dynamics with a brief slow wave response time-locked to the stimulus.

The precise timing of the late depolarization is modulated by the phase of the ongoing slow wave at the time of stimulus arrival

Visual inspection of traces shows that, for every neuron and ECoG condition, most transitions to the LD were narrowly clustered around the mean LD latency (439 ± 33 ms and 340 ± 32 ms for the slow wave and activated states, respectively; $P = 0.06$, *t* test), but the coefficients of variation of the LD (0.41 ± 0.03 and 0.20 ± 0.05 for slow wave and activated state conditions, respectively, $P = 0.003$, *t* test) and MSN V_m post-stimulus IIP distribution circular dispersion (0.32 ± 0.16 and -0.50 ± 0.24 for slow wave and activated state conditions, respectively, $P = 0.003$, *t* test) differed significantly between background ECoG conditions. We sought the source of increased LD latency variability in the slow wave condition by determining whether it depended on the phase of ongoing slow wave at the time of stimulus arrival. To that end, we plotted the time of striatal transitions to LD (radial axis) as a function of the instantaneous phase of ongoing cortical slow wave at the time of stimulus arrival (angular axis). Trials depicting LD time advances or delays were concentrated within

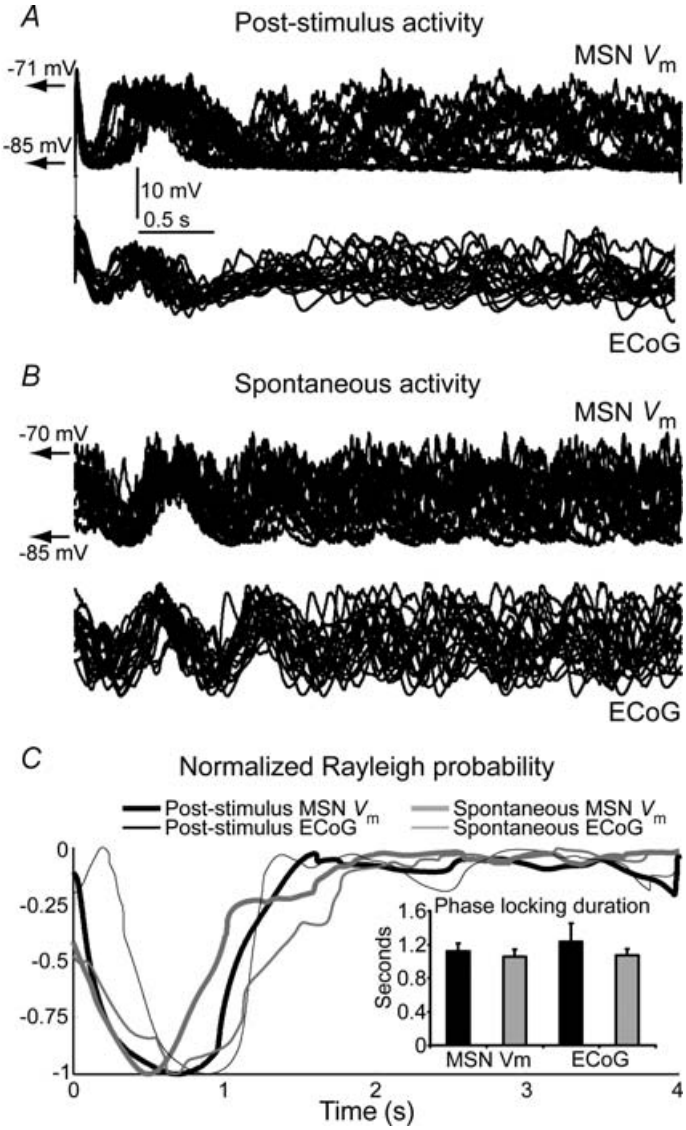

Figure 6. The shifting effect of cortical stimulation is short-lived
A, recordings aligned at stimulus onset (20 selected trials at 4 s inter-stimulus interval) of a MSN–ECoG pair showing that the phase shifting effect of cortical stimulation lasts about 1 s. *B*, twenty selected 4 s epochs of spontaneous activity of the same MSN–ECoG pair were aligned at a transition from a Down to an Up state to study the inherent variability of slow oscillations. Although traces seem aligned for the initial second, there is no obvious concentration of slow oscillation phase beyond 2 s after the aligning tag. *C*, to estimate the duration of the phase shifting effect of cortical stimulation, we computed inter-trial instantaneous phase (IIP) distributions following the stimulus and the probability of IIP distributions to be uniform with the Rayleigh test. Rayleigh probabilities were normalized (−1 to 0) and depicted as a function of post-stimulus time, for the MSN–ECoG pair illustrated above (90 trials). IIP distributions were strongly non-uniform for about 1 s after the stimulus, but Rayleigh probability increased steeply following stimulation, indicating a strong trend towards uniformity. The curves obtained with post-stimulus data and with artificially aligned spontaneous data overlapped completely. Inset: the duration of the 'phase shifting effect' was established as the time at which the Rayleigh probability increased 50% in the relative scale. There were no differences between phase shifting durations of cortical stimulation and artificially aligning spontaneous activity ($n = 6$ MSN–ECoG pairs tested with inter-stimulus intervals of 4–6 s, paired *t* test).

discrete regions of ECoG phase space (Fig. 7*B*). Within the 180–300 deg ECoG phase range, corresponding to the second half of Down states and onset of Up states in MSNs (see Fig. 4*D* and dark grey line in Fig. 7*C*), trials showing LD time advances prevailed. Conversely, stimuli arriving within the 0–90 deg ECoG phase range, corresponding to the second half of MSN Up states, had increased chances of producing delayed LDs. Remarkably, LD advances and delays occurred without changes in IPD between the ECoG and MSN V_m (Fig. 5*C*). The fact that stimulus arriving during silent or active cortical states induced advanced or delayed LDs, respectively, indicates that cortical activity at

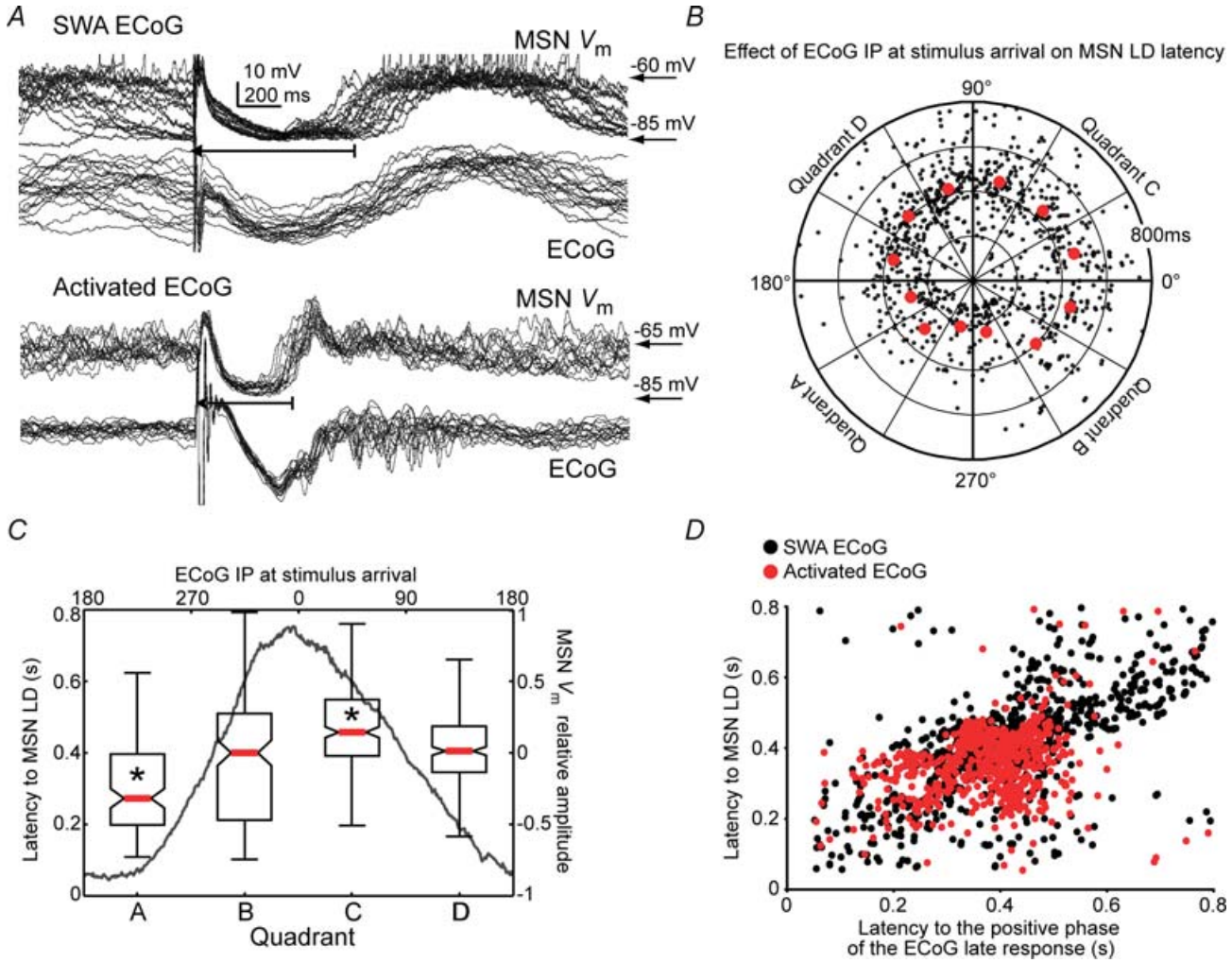

Figure 7. The precise timing of the late depolarization (LD) is determined by the ECoG phase at the time of stimulus arrival

A, overlapped trials of simultaneous MSN and ECoG responses to cortical stimulation in the slow wave (above) and activated (below) state conditions. Recordings are from different MSN. In the latter condition, a lower variability of LD latency was observed. *B*, polar plot illustrating MSN LD latency (radial axis) of individual stimulation trials ($n = 13$ MSN; 2 s inter-stimulus interval) as a function of ECoG slow oscillation instantaneous phase (IP; angular axis) at stimulus arrival. Red dots represent median values of the respective angular intervals. *C*, median LD latency (red bar), 25–75% data interval (box) and range (error bar) for the four quadrants (A, B, C and D) of the polar plot. The dark grey line is the relative amplitude of MSN membrane potential as function of ECoG IP at the time of stimulus arrival (upper *x*-axis). LD latency was smaller when cortical stimuli arrived late during the negative part of the cortical field potential, corresponding to the second half of MSN Down states (quadrant A), and increased to reach a maximum during the late part of the cortical active state (quadrant C), corresponding to the second half of MSN Up states ($P < 0.00001$, Kruskall-Wallis ANOVA; $^*P < 0.05$ *versus* any other quadrant, *post hoc* Tukey test). *D*, latency to MSN LD plotted as function of the latency to the positive component of the evoked cortical field potential, both in the slow wave (SWA ECoG) and activated ECoG (activated ECoG) conditions. Inter-trial variability was lower in activated ECoG background condition. Latencies to MSN LD and cortical positive wave displayed simultaneous inter-trial changes and were linearly related ($r = 0.49$, $P < 0.001$ for the regression's ANOVA).

the time of stimulus arrival influences the precise timing of evoked cortical and striatal slow waves. Nonetheless, the core dynamics of evoked cortical and striatal slow waves were independent of ongoing activity.

Cortical stimulation turns off cortical ensembles and striatal Up states

Delivery of an electrical pulse to the cerebral cortex can produce a LLH in MSN coupled to a negative deflection in the ECoG, regardless of slow wave phase at the time of stimulus arrival or background activity state. This implies that cortical stimulation can turn off MSN Up states (see Figs 5*A* and 7*A*). As local stimulation can turn off persistent spiking of cortical ensembles *in vitro* (Shu *et al.* 2003), it seemed likely that cortical stimulation was simultaneously turning off persistent cortical activity in the vicinity of the stimulating electrode and striatal Up states in the corresponding striatal territory in our *in vivo* experimental conditions. As the low frequency components of cortical field potentials are probably more closely related to synchronous synaptic input to cortical ensembles than to local neuronal spiking, we recorded spiking activity of cortical ensembles in the vicinity of the concentric bipolar electrode that picked up the ECoG, together with the V_m of a MSN from a connected striatal region ($n = 9$), to further understand the cortical dynamics related to MSN Up state termination and late responses. A waveform obtained after rectifying, adding and smoothing activities of the 16 probe channels (MUras) was remarkably similar to the ECoG (see Fig. 2*A*) and clearly indicated transitions between silent and active cortical states. In our experimental conditions, cortical stimulation produced a pause in local neuronal firing followed by sustained spiking, which were simultaneous with the negative and positive portions of evoked ECoG waves and the LLH and LD of MSN, regardless of the background ECoG condition ($n = 9$; 4 s inter-stimulus interval; Fig. 8). This indicates that cortical stimulation turns off cortical ensemble spiking *in vivo* concomitantly with MSN Up states.

To further study the dynamics of stimulus-induced changes in cortical ensemble firing, MUras waveforms were wavelet decomposed to obtain their low frequency components. This way, it was possible to assign an instantaneous frequency and phase (by means of a Hilbert transformation) to firing activity of a cortical ensemble. Overall, the effects of cortical stimulation on local cortical firing dynamics were similar to those induced on MSN V_m fluctuations. Cortical stimulation caused a concentration of post-stimulus IIPs of multiunit activity (Fig. 9*A*). We determined that the ECoG phase at the time of stimulus arrival had similar influence on the latency to the first post-stimulus activation of cortical ensembles and on MSN LD (Fig. 9*B*). Also, the LD latency increased linearly with increasing delays of cortical ensemble post-stimulus activation (Fig. 9*C*). These results indicate that MSN late responses replicate stimulus-induced dynamics of spiking activity in cortical ensembles they receive inputs from.

We further examined the relationship between cortical ensemble firing and spontaneous MSN Up states in the slow wave condition. Sharp increases in cortical ensemble firing were tightly coupled to transitions to the Up state, while transitions to the Down state were closely linked to spontaneous termination of persistent firing in the cortex (Fig. 10). Thus, transitions between MSN Up and Down states, either spontaneous or induced by cortical stimulation, are dictated by transitions between persistent firing and silent states in cortical ensembles.

Discussion

The temporal dynamics of the cortical control of striatal Up states within connected cortical and striatal territories were analysed *in vivo*. MSN Up states invariably end when persistent firing of cortical ensembles stops, either spontaneously or by local electrical stimulation. Cortical stimulation also causes transient phase shifts in cortical and striatal activity lasting less than 1 s. The phase perturbations introduced by cortical stimulation on MSN V_m fluctuations can be entirely explained by a post-stimulus resumption of cortical persistent firing.

Cortical stimulation elicits slow events resembling Down-to-Up state transitions in MSN independently of background cortical and striatal activities

Stimulus-related neural responses can be interpreted as partial phase shifts of ongoing neural oscillations or as transient novel neural activation (Makeig *et al.* 2002; Fell *et al.* 2004; Shah *et al.* 2004). In the former case, an oscillation with a dominant frequency similar to that of the neural response should be observed without a significant power change. In the latter, a novel frequency composition or an increase in power of an already existent oscillation should be detected. Our results show that MSN late responses have similar slow envelopes, regardless of ongoing cortical and striatal activity states, consisting of a phase perturbation of ongoing rhythms when the network is in the slow wave state or novel neural activity when the network is in the activated state. We also showed that MSN LLH occurs at the time of cortical stimulation-induced pauses in cortical ensemble spiking and that both LLH duration and cortical pauses are linearly related. Thus, our results provide strong evidence for a role of 'cortical disfacilitation' in the genesis of LLH, as proposed by Wilson *et al.* (1983). As functionally related regions of the frontal cortex and thalamus are interconnected and send

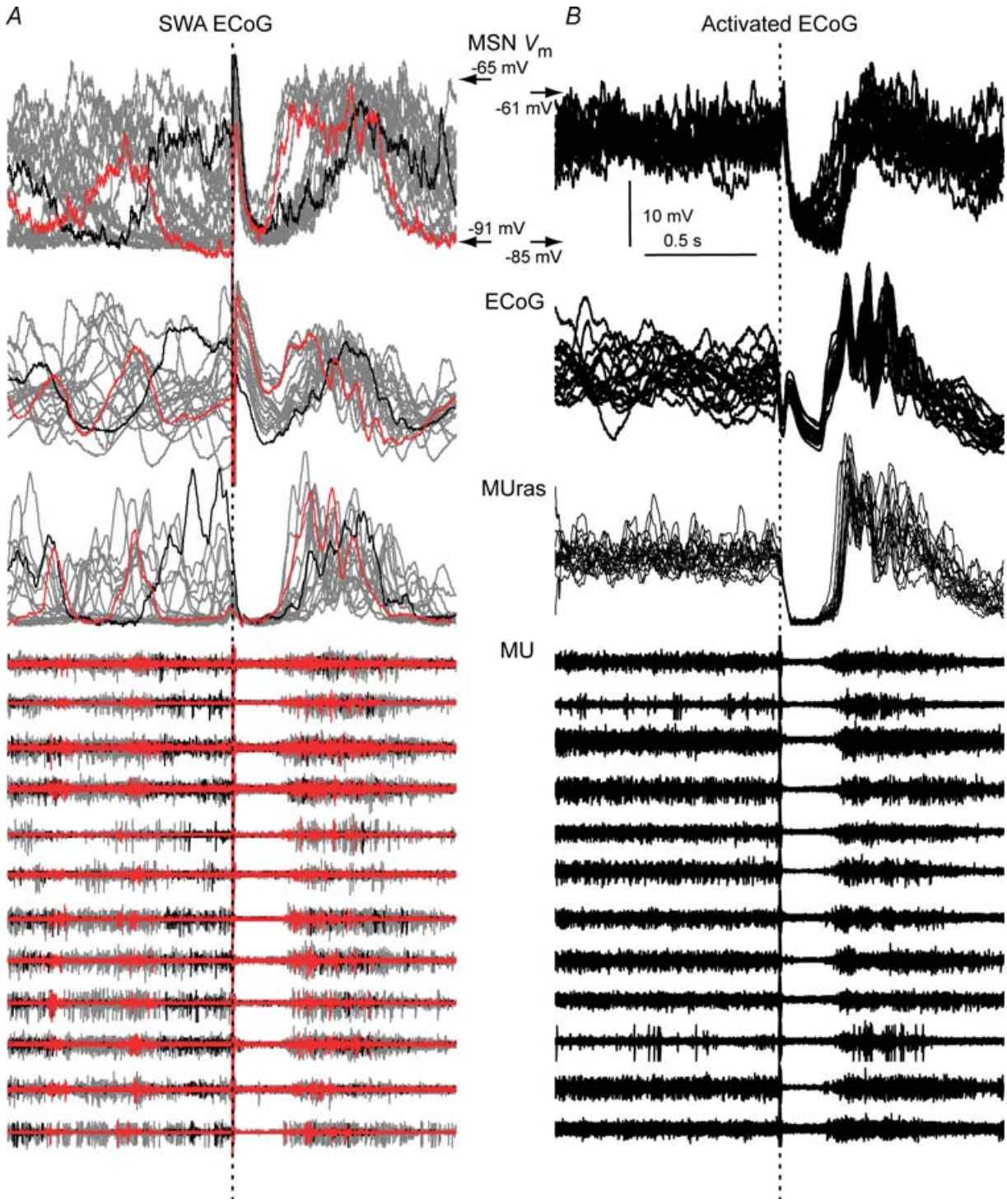

Figure 8. Cortical stimulation turns off cortical ensembles and MSN Up states
Arbitrary selected stimulation trials (inter-stimulus interval: 4 s) aligned at stimulus onset (dotted line) showing cortical firing activity (12 channels) simultaneously recorded with MSN V_m, during the slow wave (*A,* 20 trials) and activated state (*B,* 20 trials) conditions. A waveform representing the activity of all active multi-unit channels after rectification, addition and smoothing (MUras), and the ECoG, are also displayed. A pause in firing takes place in all MU channels coincident with the negative phase of the ECoG wave and the MSN LLH. In the slow wave condition (*A*), latencies to evoked active states were shorter if stimuli arrived during silent (red traces) than during active (black traces) states. In *A*, two trials were coloured to illustrate the relationship between timing of stimulus arrival relative to ongoing activity and LD latency.

convergent inputs to functionally related striatal territories (reviewed by Smith *et al.* 2004), a contribution of antidromic invasion of thalamocortical axons in the generation of dPSP in MSNs and of orthodromic activation of the thalamus by cortical input in determining the dynamics of the MSN late response cannot be denied.

Cortical stimulation turns off cortical ensembles

Neuronal ensembles in the isolated cerebral cortex can display spontaneous episodes of persistent spiking activity, which are sustained by recurrent excitatory and inhibitory connections and promoted by dopamine (Sanchez-Vives & McCormick, 2000; Timofeev *et al.* 2000; Cossart

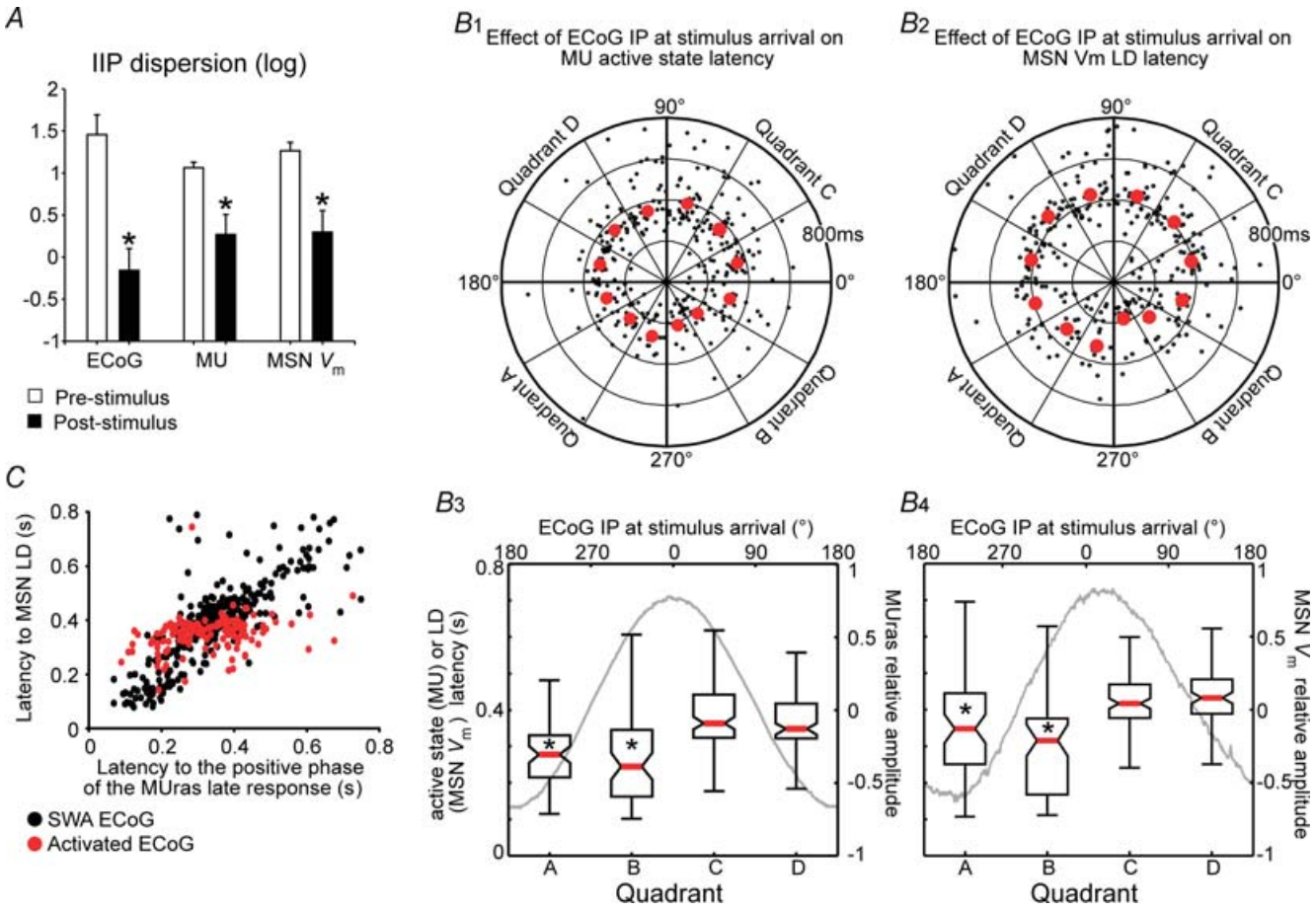

Figure 9. Post-stimulus resumption of cortical persistent firing dictates the dynamics of MSN late response to cortical stimulation

A, to examine the phase shifting effect of cortical stimulation in the slow wave condition ($n = 8$, 4 s inter-stimulus interval, 25–100 trials per neuron), we computed inter-trial instantaneous phase (IIP) distributions for the simultaneously recorded ECoG, MUras and MSN V_m, and took circular dispersion of IIP distributions as a measure of stimulus-induced phase concentration. IIP circular dispersion fell dramatically following stimulation in all three recordings (*$P < 0.001$ *versus* pre-stimulus, *t* test for paired data). *B*, polar plots illustrating the latencies to the first post-stimulus persistent cortical firing episode (*B*1) or to the MSN LD (*B*2) as a function of ECoG phase at stimulus arrival ($n = 8$ MUras–MSN pairs, 4 s inter-stimulus interval). The latency to cortical ensemble activation was computed from wavelet decomposed and normalized MUras, as the time to the first negative-to-positive post-stimulus waveform transition. Polar plot data are summarized in the box and whisker graphs below, showing median latency (red bar), 25–75% data interval (box) and range (error bar) for the four quadrants (A, B, C and D) of the corresponding polar plots. Grey lines are MUras waveform (*B*3) or MSN membrane potential (*B*4) mean relative amplitudes as a function of ECoG IP at the time of stimulus arrival (upper *x*-axis) ($P < 0.00001$, Kruskall-Wallis ANOVA; *$P < 0.05$ *versus* quadrants C and D, *post hoc* Tukey test). *C*, latency of MSN LD plotted as a function of the latency of cortical ensemble activation in slow wave ($n = 8$ MUras–ECoG pairs, black circles) and activated ECoG conditions ($n = 4$ MUras–ECoG pairs, red circles). LD latency increased linearly with increasing cortical ensemble activation delay ($r = 0.81$, $P < 0.001$ for the regression's ANOVA). One MUras–MSN pair could be recorded in the activated ECoG condition only.

et al. 2003; Tseng & O'Donnell, 2005). Local electrical stimulation may activate or suppress persistent cortical activity, depending on stimulus intensity and timing relative to the initiation of persistent firing episodes, in cortical slices (Shu *et al.* 2003). In this preparation, high intensity stimuli arriving late during active network states could preferentially activate inhibitory interneurons, increasing the probability of silencing the network. In our *in vivo* experiments cortical stimulation did not elicit persistent cortical activity, but led to cortical inactivation. This is in good agreement with reports showing that cortical stimulation may trigger active states in cortical slabs but not in the intact brain (Timofeev *et al.* 2000). Although extracellular recordings do not allow unequivocal identification of recorded cell types, systemic $GABA_A$ receptor antagonists reduce MSN LLH more effectively than via intrastriatal administration (Calabresi *et al.* 1990). This suggests that cortical inhibitory circuits can contribute to turning off cortical and striatal persistent activity *in vivo*.

There is a debate as to whether MSN can exhibit bi-stable activity (Nicola *et al.* 2000). When striatal MSN are recorded *in vitro* or in isolation, spontaneous persistent activity cannot be observed. Up state transitions do not occur in the dorsal striatum of decorticated animals (Wilson, 1993) or in the nucleus accumbens after fornix transection (O'Donnell & Grace, 1995), and cannot be induced by depolarizing current pulses or single-pulse cortical stimulation in slices (O'Donnell & Grace, 1994, 1996). Furthermore, blocking intrinsic inward currents that could sustain MSN Up states does not eliminate spontaneous Up states *in vivo* (Wilson & Kawaguchi, 1996). These results suggest that MSN Up states are initiated and sustained by excitatory (mainly cortical) inputs. However, corticostriatal neuron firing takes place mainly during the first 200 ms of cortical slow waves and striatal Up states often last longer (Mahon *et al.* 2001). Together with this synchronized corticostriatal barrage, local GABA inputs may depolarize MSN from the Down state and contribute to initiating plateau depolarizations (Czubayko & Plenz, 2002; Blackwell *et al.* 2003; Bracci & Panzeri, 2006). It has been suggested that once Up states are initiated, their duration can be influenced by intrinsic voltage-dependent currents (Surmeier & Kitai, 1993, 1991; Galarraga *et al.* 1994). Brief depolarizing pulses can induce plateau depolarizations in slices in the presence of D_1/D_5 dopamine agonists, through a mechanism involving voltage-dependent calcium channels (Hernandez-Lopez *et al.* 1997). More recently, Vergara *et al.* (2003) reported that brief cortical stimulation can evoke slow oscillations resembling Up states in MSN. These studies suggest that striatal network interactions and intrinsic cell mechanisms can extend the time course of striatal Up states beyond that of cortical ensemble firing. Our experiments showed that cortical ensemble activity suppression (spontaneous or stimulus-induced) is invariably associated with the termination of MSN Up states in anaesthetized animals. The effect of cortical stimulation was not dependent on background brain activity or on the time of stimulus arrival relative to ongoing slow oscillation phase (i.e. MSN Up state duration prior to stimulation). A recent computational model using intrinsic conductance values obtained from real recordings could not produce MSN Up states unless persistent cortical inputs and an appropriate NMDA/AMPA ratio was added (Wolf *et al.* 2005). Furthermore, *in vivo* recordings from MSN while delivering intracellular current injection failed to affect Up–Down transitions (O'Donnell & Grace, 1995; Wilson & Kawaguchi, 1996; Charpier *et al.* 1999), suggesting that voltage-dependent conductances play a minor role *in vivo*.

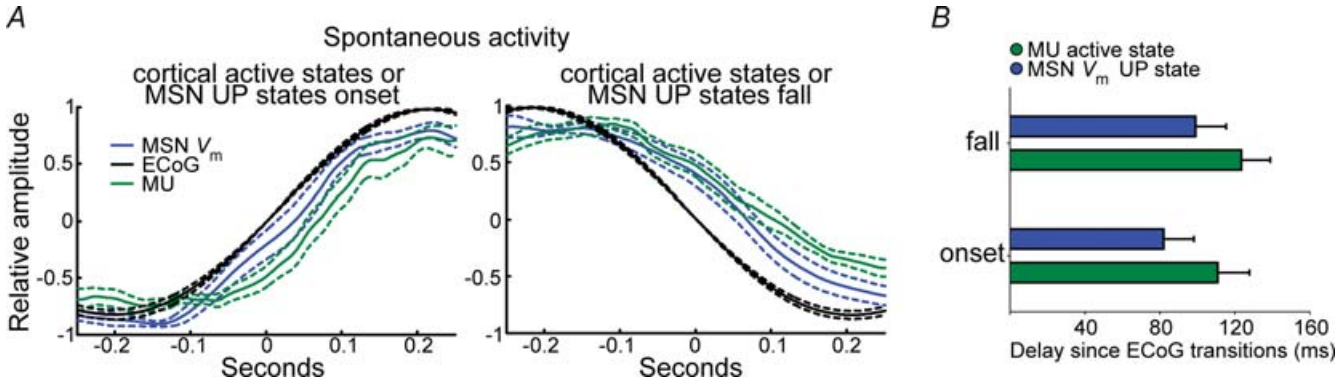

Figure 10. Spontaneous transitions between Up and Down states in striatal MSN are tightly coupled to transitions between active and silent states in cortical ensembles
A, 500-ms-long segments of normalized MUras (green) and MSN V_m (blue) were aligned at the time of spontaneous transitions to the positive (left) and negative (right) parts of normalized 0.5–2 Hz wavelet decomposed ECoG slow waves (black), and averaged and displayed with their S.D. ($n = 8$, 30 s of signal for each neuron). *B*, time lag from ECoG transitions to MUras and MSN V_m transitions (mean ± S.E.M., $n = 8$). Transitions between spiking and silent states took place almost simultaneously in cortical ensembles and MSN in all recorded pairs.

Of course, in these and other similar experiments, space clamp limitations preclude ruling out a contribution of distal dendritic currents to MSN Up states. However, our present results unequivocally establish that MSN Up states do not persist in the absence of cortical ensemble firing *in vivo*.

Another element that needs to be considered is the potential role of striatal fast spiking interneurons (FSI) in ending stimulation-induced MSN Up states. Striatal FSI respond to cortical stimulation more strongly and at lower intensities than MSN do (Mallet *et al.* 2005) and induce fast $GABA_A$ receptor-mediated IPSPs when MSN are in the Up state (Plenz & Kitai, 1998; Koos & Tepper, 1999; Blackwell *et al.* 2003). Therefore, FSI-mediated intra-striatal inhibition and passive membrane properties could counterbalance any effect of voltage-dependent membrane currents, forcing MSN to the Down state when persistent cortical firing falls below a critical threshold.

MSN membrane potential fluctuation remains phase-locked to cortical ensemble spiking after stimulus-induced perturbations of cortical dynamics

Persistent activity in cortical ensembles occurs spontaneously across different brain activity states and can be phase-modulated by afferent inputs. Its slowest frequency components may bind distributed neuronal networks and set the timing for high frequency oscillations to be transmitted through neuronal ensembles. Therefore, concerted fast phase modulations of low frequency oscillations may be essential for communication among brain regions (Steriade, 2000; Varela *et al.* 2001; Engel *et al.* 2001; Buzsaki & Draguhn, 2004). In this context, we explored whether phase perturbations of cortical activity impact on dorsal striatal MSN physiology, showing that cortical stimulation produces almost simultaneous phase perturbations of ongoing slow wave activity in cortical networks and in MSN. A short delay between the activity of cortical ensembles and MSN V_m is conserved throughout the LD as well as during spontaneous Up–Down alternation. Furthermore, during cortical activation, cortical stimulation induces a slow MSN V_m modulation tightly phase-locked to the activity evoked in cortical ensembles. The sole remarkable difference among MSN late responses evoked during slow wave or activated states was the higher LD latency variability in the slow wave condition. Such variability was present in cortical responses to local stimulation and was related to the phase of ongoing slow waves at the time of stimulus arrival. Our results indicate that MSN LD dynamics can be entirely explained by effects of local electrical stimulation on cortical activity. After being turned off by the stimulus, cortical ensembles may resume persistent activity impelling MSN in connected striatal territories into the Up state.

Functional implications

Definitive evidence of the occurrence of MSN Up–Down state transitions in behavioural contexts is still lacking. Theoretical speculations about MSN subthreshold activity in behavioural contexts perceive Up states as time gates during which MSN can fire action potentials in response to specific cortical inputs. Indeed, previous studies revealed that synchronous activation of hippocampal afferents induce transitions to the Up state in nucleus accumbens MSN, which fire action potentials in response to prefrontal cortical stimulation only during these hippocampal-driven plateau depolarizations (O'Donnell & Grace, 1995). Dorsal striatal MSN are impelled to the Up state by neocortical neurons and presumably fire action potentials in response to specific input embedded within a broad neocortical signal (Stern *et al.* 1998). We and others have reported that spontaneous transitions between Up and Down states in MSN are driven by cortical slow waves (Charpier *et al.* 1999; Goto & O'Donnell, 2001; Mahon *et al.* 2001; Tseng *et al.* 2001; Kasanetz *et al.* 2002; Goldberg *et al.* 2003) and that cortical activated states are associated with non-rhythmic MSN depolarizations (Mahon *et al.* 2001; Kasanetz *et al.* 2002). The present results extend these findings by demonstrating a precise alignment between MSN Up states and episodes of persistent cortical activity within connected cortical and dorsal striatum territories. It is important to note that, even though we provided direct functional evidence of connections between the recorded cortical and striatal territories, most of the recorded cortical units were probably not corticostriatal neurons. This establishes a difference from previous studies focused on corticostriatal neuron activity which revealed that single corticostriatal neurons display Up states and fire at specific times during cortical slow waves (Stern *et al.* 1997; Charpier *et al.* 1999; Mahon *et al.* 2001). Therefore, our findings truly imply that MSN Up states are representations of persistent firing in cortical ensembles that would be involved in local computations and influence extra-striatal targets as well. Besides, our findings indicate that corticostriatal neuron activity alone or in conjunction with indirect connections between the cortex and striatum (for example, via functionally related thalamic nuclei) transmit a reliable depiction of cortical ensemble activity to the striatum, as postulated in theoretical models (Houk & Wise, 1995; Graybiel, 1998; Redgrave *et al.* 1999; Bar-Gad *et al.* 2003). The precise alignment between episodes of persistent cortical firing and striatal Up states would let MSN detect specific discharge patterns embedded within the more general cortical input that dictates Up state transitions and duration. This could allow MSN to detect coincident cortical events for estimating time (Matell & Meck, 2004), for example, or encoding singular events during the execution of learned behavioural sequences (Fujii & Graybiel, 2005).

References

Bar-Gad I, Morris G & Bergman H (2003). Information processing, dimensionality reduction and reinforcement learning in the basal ganglia. *Prog Neurobiol* **71**, 439–473.

Blackwell KT, Czubayko U & Plenz D (2003). Quantitative estimate of synaptic inputs to striatal neurons during up and down states in vitro. *J Neurosci* **23**, 9123–9132.

Bracci E & Panzeri S (2006). Excitatory GABAergic effects in striatal projection neurons. *J Neurophysiol* **95**, 1285–1290.

Buzsaki G & Draguhn A (2004). Neuronal oscillations in cortical networks. *Science* **304**, 1926–1929.

Calabresi P, Mercuri NB, Stefani A & Bernardi G (1990). Synaptic and intrinsic control of membrane excitability of neostriatal neurons. I. An in vivo analysis. *J Neurophysiol* **63**, 651–662.

Charpier S, Mahon S & Deniau JM (1999). In vivo induction of striatal long-term potentiation by low-frequency stimulation of the cerebral cortex. *Neuroscience* **91**, 1209–1222.

Cossart R, Aronov D & Yuste R (2003). Attractor dynamics of network UP states in the neocortex. *Nature* **423**, 283–288.

Czubayko U & Plenz D (2002). Fast synaptic transmission between striatal spiny projection neurons. *Proc Natl Acad Sci U S A* **99**, 15764–15769.

Engel AK, Fries P & Singer W (2001). Dynamic predictions: oscillations and synchrony in top-down processing. *Nat Rev Neurosci* **2**, 704–716.

Fell J, Dietl T, Grunwald T, Kurthen M, Klaver P, Trautner P, Schaller C, Elger CE & Fernandez G (2004). Neural bases of cognitive ERPs: more than phase reset. *J Cogn Neurosci* **16**, 1595–1604.

Fisher NI (1993). *Statistical Analysis of Circular Data*. Cambridge University Press, Cambridge, UK.

Fujii N & Graybiel AM (2005). Time-varying covariance of neural activities recorded in striatum and frontal cortex as monkeys perform sequential-saccade tasks. *Proc Natl Acad Sci U S A* **102**, 9032–9037.

Galarraga E, Pacheco-Cano MT, Flores-Hernandez JV & Bargas J (1994). Subthreshold rectification in neostriatal spiny projection neurons. *Exp Brain Res* **100**, 239–249.

Goldberg JA, Kats SS & Jaeger D (2003). Globus pallidus discharge is coincident with striatal activity during global slow wave activity in the rat. *J Neurosci* **23**, 10058–10063.

Goto Y & O'Donnell P (2001). Synchronous activity in the hippocampus and nucleus accumbens in vivo. *J Neurosci* **21**, RC131, 1–5.

Graybiel AM (1998). The basal ganglia and chunking of action repertoires. *Neurobiol Learn Mem* **70**, 119–136.

Gruber AJ, Solla SA, Surmeier DJ & Houk JC (2003). Modulation of striatal single units by expected reward: a spiny neuron model displaying dopamine-induced bistability. *J Neurophysiol* **90**, 1095–1114.

Hernandez-Lopez S, Bargas J, Surmeier DJ, Reyes A & Galarraga E (1997). D1 receptor activation enhances evoked discharge in neostriatal medium spiny neurons by modulating an L-type Ca^{2+} conductance. *J Neurosci* **17**, 3334–3342.

Houk JC & Wise SP (1995). Distributed modular architectures linking basal ganglia, cerebellum, and cerebral cortex: their role in planning and controlling action. *Cereb Cortex* **5**, 95–110.

Kasanetz F, Riquelme LA & Murer MG (2002). Disruption of the two-state membrane potential of striatal neurones during cortical desynchronisation in anaesthetised rats. *J Physiol* **543**, 577–589.

Kita H & Armstrong W (1991). A biotin-containing compound N-(2-aminoethyl) biotinamide for intracellular labeling and neuronal tracing studies: comparison with biocytin. *J Neurosci Meth* **37**, 141–150.

Koos T & Tepper JM (1999). Inhibitory control of neostriatal projection neurons by GABAergic interneurons. *Nat Neurosci* **2**, 467–472.

Lewis BL & O'Donnell P (2000). Ventral tegmental area afferents to the prefrontal cortex maintain membrane potential 'up' states in pyramidal neurons via D_1 dopamine receptors. *Cereb Cortex* **10**, 1168–1175.

Mahon S, Deniau JM & Charpier S (2001). Relationship between EEG potentials and intracellular activity of striatal and cortico-striatal neurons: an in vivo study under different anesthetics. *Cereb Cortex* **11**, 360–373.

Major G & Tank D (2004). Persistent neural activity: prevalence and mechanisms. *Curr Opin Neurobiol* **14**, 675–684.

Makeig S, Westerfield M, Jung TP, Enghoff S, Townsend J, Courchesne E & Sejnowski TJ (2002). Dynamic brain sources of visual evoked responses. *Science* **295**, 690–694.

Mallet N, Le Moine C, Charpier S & Gonon F (2005). Feedforward inhibition of projection neurons by fast-spiking GABA interneurons in the rat striatum in vivo. *J Neurosci* **25**, 3857–3869.

Matell MS & Meck WH (2004). Cortico-striatal circuits and interval timing: coincidence detection of oscillatory processes. *Cogn Brain Res* **21**, 139–170.

Meyer Y (1992). Wavelets and operators. In *Cambridge Studies in Advanced Mathematics*, no. 37. Cambridge University Press, Cambridge, UK.

Nicola SM, Surmeier J & Malenka RC (2000). Dopaminergic modulation of neuronal excitability in the striatum and nucleus accumbens. *Annu Rev Neurosci* **23**, 185–215.

O'Donnell P & Grace AA (1994). Tonic D2-mediated attenuation of cortical excitation in nucleus accumbens neurons recorded in vitro. *Brain Res* **634**, 105–112.

O'Donnell P & Grace AA (1995). Synaptic interactions among excitatory afferents to nucleus accumbens neurons: hippocampal gating of prefrontal cortical input. *J Neurosci* **15**, 3622–3639.

O'Donnell P & Grace AA (1996). Dopaminergic reduction of excitability in nucleus accumbens neurons recorded in vitro. *Neuropsychopharmacol* **15**, 87–97.

Oppenheim AV, Schafer RW & Buck CK (1999). *Discrete-Time Signal Processing*, 2nd edn. Prentice Hall, Englewood Cliffs, NJ, USA.

Paxinos G & Watson C (1997). The rat brain in stereotaxic coordinates, 3rd edn. Academic, London.

Plenz D & Kitai ST (1998). Up and down states in striatal medium spiny neurons simultaneously recorded with spontaneous activity in fast-spiking interneurons studied in cortex-striatum-substantia nigra organotypic cultures. *J Neurosci* **18**, 266–283.

Redgrave P, Prescott TJ & Gurney K (1999). The basal ganglia: a vertebrate solution to the selection problem? *Neuroscience* **89**, 1009–1023.

Sanchez-Vives MV & McCormick DA (2000). Cellular and network mechanisms of rhythmic recurrent activity in neocortex. *Nat Neurosci* **3**, 1027–1034.

Shah AS, Bressler SL, Knuth KH, Ding M, Mehta AD, Ulbert I & Schroeder CE (2004). Neural dynamics and the fundamental mechanisms of event-related brain potentials. *Cereb Cortex* **14**, 476–483.

Shu Y, Hasenstaub A & McCormick DA (2003). Turning on and off recurrent balanced cortical activity. *Nature* **423**, 288–293.

Smith Y, Raju DV, Pare JF & Sidibe M (2004). The thalamostriatal system: a highly specific network of the basal ganglia circuitry. *Trends Neurosci* **27**, 520–527.

Steriade M (2000). Corticothalamic resonance, states of vigilance and mentation. *Neuroscience* **101**, 243–276.

Stern EA, Jaeger D & Wilson CJ (1998). Membrane potential synchrony of simultaneously recorded striatal spiny neurons in vivo. *Nature* **394**, 475–478.

Stern EA, Kincaid AE & Wilson CJ (1997). Spontaneous subthreshold membrane potential fluctuations and action potential variability of rat corticostriatal and striatal neurons in vivo. *J Neurophysiol* **77**, 1697–1715.

Suri RE, Bargas J & Arbib MA (2001). Modeling functions of striatal dopamine modulation in learning and planning. *Neuroscience* **103**, 65–85.

Surmeier DJ & Kitai ST (1993). D1 and D2 dopamine receptor modulation of sodium and potassium currents in rat neostriatal neurons. *Prog Brain Res* **99**, 309–324.

Timofeev I, Grenier F, Bazhenov M, Sejnowski TJ & Steriade M (2000). Origin of slow cortical oscillations in deafferented cortical slabs. *Cereb Cortex* **10**, 1185–1199.

Tseng KY, Kasanetz F, Kargieman L, Riquelme LA & Murer MG (2001). Cortical slow oscillatory activity is reflected in the membrane potential and spike trains of striatal neurons in rats with chronic nigrostriatal lesions. *J Neurosci* **21**, 6430–6439.

Tseng KY & O'Donnell P (2005). Post-pubertal emergence of prefrontal cortical up states induced by D_1-NMDA co-activation. *Cereb Cortex* **15**, 49–57.

Tseng KY, Riquelme LA & Murer MG (2004). Impact of D1-class dopamine receptor on striatal processing of cortical input in experimental parkinsonism in vivo. *Neuroscience* **123**, 293–298.

Varela F, Lachaux JP, Rodriguez E & Martinerie J (2001). The brainweb: phase synchronization and large-scale integration. *Nat Rev Neurosci* **2**, 229–239.

Vergara R, Rick C, Hernandez-Lopez S, Laville JA, Guzman JN, Galarraga E, Surmeier DJ & Bargas J (2003). Spontaneous voltage oscillations in striatal projection neurons in a rat corticostriatal slice. *J Physiol* **553**, 169–182.

Voorn P, Vanderschuren LJ, Groenewegen HJ, Robbins TW & Pennartz CM (2004). Putting a spin on the dorsal-ventral divide of the striatum. *Trends Neurosci* **27**, 468–474.

Wilson CJ (1993). The generation of natural firing patterns in neostriatal neurons. *Prog Brain Res* **99**, 277–297.

Wilson CJ, Chang HT & Kitai ST (1983). Disfacilitation and long-lasting inhibition of neostriatal neurons in the rat. *Exp Brain Res* **51**, 227–235.

Wilson CJ & Kawaguchi Y (1996). The origins of two-state spontaneous membrane potential fluctuations of neostriatal spiny neurons. *J Neurosci* **16**, 2397–2410.

Wolf JA, Moyer JT, Lazarewicz MT, Contreras D, Benoit-Marand M, O'Donnell P & Finkel LH (2005). NMDA/AMPA ratio impacts state transitions and entrainment to oscillations in a computational model of the nucleus accumbens medium spiny projection neuron. *J Neurosci* **25**, 9080–9095.

Yuste R, MacLean JN, Smith J & Lansner A (2005). The cortex as a central pattern generator. *Nat Rev Neurosci* **6**, 477–483.

Acknowledgements

This study was supported by NIH Research Grant R03 TW6282 (P.O'D.) funded by the Fogarty International Center and the National Institute on Mental Health (USA), Secretaría de Ciencia, Tecnología e Innovación Productiva, Fondo para la Investigación Científica y Tecnológica (FONCYT, Argentina; PICT2002-05-11012; PME2003-29), Universidad de Buenos Aires (UBACYT M056) y Consejo Nacional de Investigaciones Científicas y Técnicas (Argentina), and National Parkinson Foundation, USA (M.G.M.). We thank the University of Michigan Center for Neural Communication Technology sponsored by NIH/NCRR grant P41 RR09754 for providing the silicon probes used in this study. We would like to thank Dr Aaron Gruber for helpful comments.

Supplemental material

The online version of this paper can be accessed at:
DOI: 10.1113/jphysiol.2006.113050
http://jp.physoc.org/cgi/content/full/jphysiol.2006.113050/DC1
and contains one supplemental figure: Electrical stimulation of non-matched cortical regions elicits dDPSP and late responses in MSN.

This material can also be found as part of the full-text HTML version available from http://www.blackwell-synergy.com